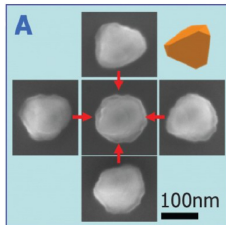


Bayesian shape inversion in acoustic scattering

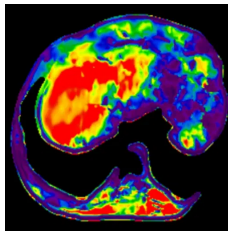
Laura Scarabosio, Safiere Kuijpers

Uncertainty Quantification for High-Dimensional Problems
14 November 2024, CWI Amsterdam

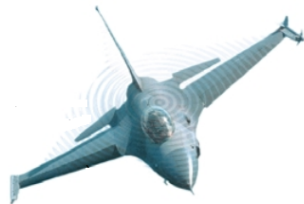
Inverse scattering in applications



Sannomiya, Diss. ETHZ 18747



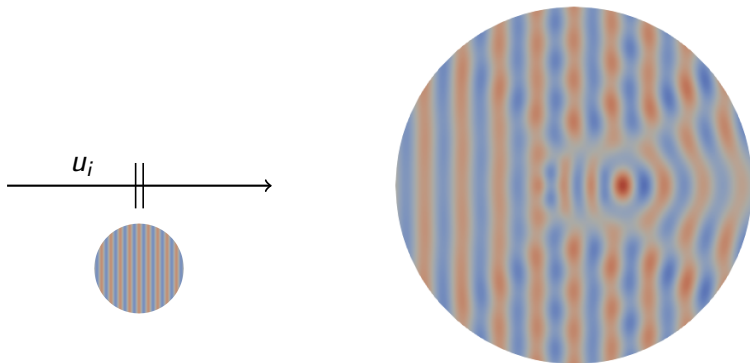
siemens-healthineers.com



Borden, Inverse Problems (2002)

We consider reconstructing a **shape** in **time-harmonic** scattering.

Situation sketch



Goal: infer scatterer's shape from measurements of the scattered field.

Focus: effect of the frequency on the inversion result.

Bayesian shape inverse problem

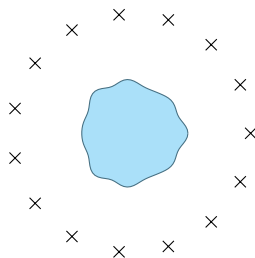
Assumptions

star-shaped scatterer

non-trapping regime [Moiola, Spence 2017]

finite dimensional measurements

additive noise $\boldsymbol{\eta} \sim \mathcal{N}(\mathbf{0}, \Sigma)$



Given a prior measure μ_0 on r , find the posterior μ^δ given the observations

$$\delta = \mathcal{G}(r) + \boldsymbol{\eta},$$

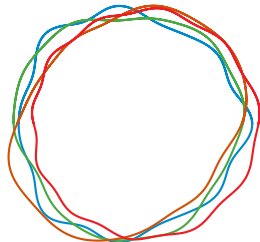
Plan

- Shape prior
- Forward model
- Frequency-explicit well-posedness
- Posterior sampling
- Numerical results

Shape prior

Key tool: random field

for:
domain deformations
normal displacement
boundary function
level set



We use the model:

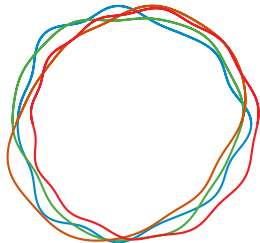
$$r(\omega; \varphi) = r_0(\varphi) + \sum_{j=1}^d \beta_j Y_j(\omega) \psi_j(\varphi)$$

where $Y_j \sim \mathcal{U}([-1, 1])$ independent, $\sum_{j \geq 1} |\beta_j| \leq \gamma_\beta \inf_\varphi r_0(\varphi)$.

Shape prior

Key tool: random field

for:
domain deformations
normal displacement
boundary function
level set



We use the model:

$$r(\omega; \varphi) = r_0(\varphi) + \sum_{j=1}^d \beta_j Y_j(\omega) \psi_j(\varphi)$$

where $Y_j \sim \mathcal{U}([-1, 1])$ independent, $\sum_{j \geq 1} |\beta_j| \leq \gamma_\beta \inf_{\varphi} r_0(\varphi)$.

Properties of the shape prior

$$r(\omega; \varphi) = r_0(\varphi) + \sum_{j=1}^d \beta_j Y_j(\omega) \psi_j(\varphi)$$

Choices for $\{\psi_j\}_j$:

Laplace-Beltrami eigenfunctions [Church et al. 2020]

Localized supports - wavelets [van Harten, S. 2024]

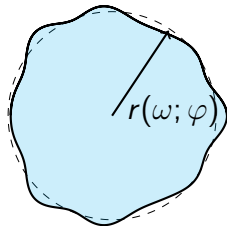
Coefficients $\{\beta_j\}_j$:

asymptotic decay \longleftrightarrow smoothness

preasymptotic decay \longleftrightarrow correlation length

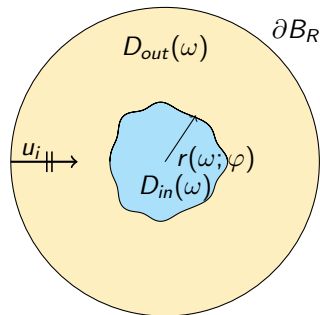
Example:

$$r(\omega; \varphi) = r_0 + \frac{r_0}{4} \sum_{j=1}^{d/2} \frac{1}{1 + \ell j^p} (Y_{2j-1}(\omega) \cos(j\varphi) + Y_{2j}(\omega) \sin(j\varphi))$$



Helmholtz transmission problem

$$\left\{ \begin{array}{l} -\alpha_{in}\Delta(u + u_i) - \kappa_0^2 n_{in}(u + u_i) = 0 \text{ in } D_{in}(\omega) \\ -\alpha_{out}\Delta(u + u_i) - \kappa_0^2 n_{out}(u + u_i) = 0 \text{ in } D_{out}(\omega) \\ + \text{continuity conditions at interface} \\ + \text{radiation condition on } u \text{ at } \partial B_R \end{array} \right.$$



Non-trapping assumption [Moiola, Spence 2019]: $\frac{n_{in}}{n_{out}} \leq \frac{\alpha_{in}}{\alpha_{out}}$

$$\mathcal{G}(r) = \mathcal{O} \circ G(r), \text{ where } G(r) = u$$

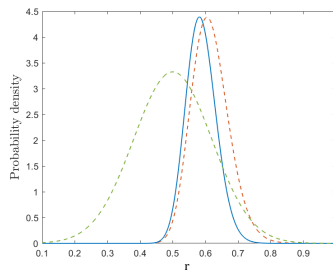
The Bayesian inverse problem

We look for probability distribution for $r = r(\omega, \varphi)$.

Bayes' rule

posterior \propto likelihood \cdot prior

$$\pi(r|\delta) \propto L(\delta|r) \cdot \pi_0(r)$$



Statistical model: $\delta = \mathcal{G}(r) + \eta$

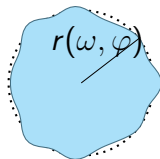
assuming $\eta \sim \mathcal{N}(0, \Sigma) \Rightarrow L(\delta|r) \propto \exp\left(-\frac{1}{2}\|\delta - \mathcal{G}(r)\|_{\Sigma}^2\right)$

The Bayesian shape inverse problem

Prior

$$r(\omega; \varphi) = r_0(\varphi) + \sum_{j=1}^d \beta_j Y_j(\omega) \psi_j(\varphi)$$

with $Y_j \sim \mathcal{U}([-1, 1])$ independent.



Frequency-explicit well-posedness [Kuijpers, S. 2024]

Existence and uniqueness

Posterior is absolutely continuous w.r.t. prior

Stability

Posterior depends continuously on the data **with constant $\sim \kappa_0 R$**

Bayesian inversion: frequency-explicit well-posedness

Theorem (Kuijpers, S. 2024)

Case 1: r is μ_0 -a.s. Lipschitz, $\alpha_{in} = \alpha_{out}$, $\frac{n_{in}}{n_{out}} < 1$ and $V = H^1(B_R)$

Bayesian inversion: frequency-explicit well-posedness

Theorem (Kuijpers, S. 2024)

Case 1: r is μ_0 -a.s. Lipschitz, $\alpha_{in} = \alpha_{out}$, $\frac{n_{in}}{n_{out}} < 1$ and $V = H^1(B_R)$

Case 2: r is μ_0 -a.s. of class $C^{2,1}$, $\frac{n_{in}}{n_{out}} < 1 < \frac{\alpha_{in}}{\alpha_{out}}$ and $V = H^1(B_R \setminus U)$.

Bayesian inversion: frequency-explicit well-posedness

Theorem (Kuijpers, S. 2024)

Case 1: r is μ_0 -a.s. Lipschitz, $\alpha_{in} = \alpha_{out}$, $\frac{n_{in}}{n_{out}} < 1$ and $V = H^1(B_R)$

Case 2: r is μ_0 -a.s. of class $C^{2,1}$, $\frac{n_{in}}{n_{out}} < 1 < \frac{\alpha_{in}}{\alpha_{out}}$ and $V = H^1(B_R \setminus U)$.

Then:

(i) $\mu^\delta \ll \mu_0$ with likelihood $L(\delta|r) \propto \exp\left(-\frac{1}{2}\|\delta - \mathcal{G}(r)\|_\Sigma^2\right)$

Bayesian inversion: frequency-explicit well-posedness

Theorem (Kuijpers, S. 2024)

Case 1: r is μ_0 -a.s. Lipschitz, $\alpha_{in} = \alpha_{out}$, $\frac{n_{in}}{n_{out}} < 1$ and $V = H^1(B_R)$

Case 2: r is μ_0 -a.s. of class $C^{2,1}$, $\frac{n_{in}}{n_{out}} < 1 < \frac{\alpha_{in}}{\alpha_{out}}$ and $V = H^1(B_R \setminus U)$.

Then:

(i) $\mu^\delta \ll \mu_0$ with likelihood $L(\delta|r) \propto \exp\left(-\frac{1}{2}\|\delta - \mathcal{G}(r)\|_\Sigma^2\right)$

(ii) for each $\gamma > 0$ s.t. $|\delta|, |\delta'| \leq \gamma$,

$$d_{\text{Hell}}(\mu^\delta, \mu^{\delta'}) \leq C \|u_i\|_{H_{\kappa_0, \alpha, n}^1(B_R)} |\delta - \delta'| \sim (\kappa_0 R) |\delta - \delta'|$$

Main tools: shape calculus (i) and estimates from [Moiola, Spence 2019] (ii).

Frequency-explicit well-posedness: remarks

Theorem (Kuijpers, S. 2024)

Case 1: r is μ_0 -a.s. Lipschitz, $\alpha_{in} = \alpha_{out}$, $\frac{n_{in}}{n_{out}} < 1$ and $V = H^1(B_R)$

Case 2: r is μ_0 -a.s. of class $C^{2,1}$, $\frac{n_{in}}{n_{out}} < 1 < \frac{\alpha_{in}}{\alpha_{out}}$ and $V = H^1(B_R \setminus U)$.

Then:

(i) $\mu^\delta \ll \mu_0$ with likelihood $L(\delta|r) \propto \exp\left(-\frac{1}{2}\|\delta - \mathcal{G}(r)\|_\Sigma^2\right)$

(ii) for each $\gamma > 0$ s.t. $|\delta|, |\delta'| \leq \gamma$,

$$d_{\text{Hell}}(\mu^\delta, \mu^{\delta'}) \leq C \|u_i\|_{H^1_{\kappa_0, \alpha, n}(B_R)} |\delta - \delta'| \sim (\kappa_0 R) |\delta - \delta'|$$

Frequency dictates the lengthscale

Constants depend on the inverse problem setting (prior, measurements)

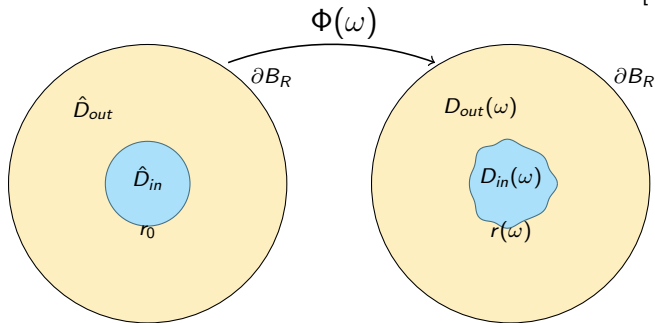
High frequency and/or high contrast worsen stability

For $\alpha_{in} = \alpha_{out}$, wider class of measurements allowed

Numerical realization: forward solver

Random PDE on *fixed* geometry \longleftrightarrow *Fixed* PDE on *random* geometry

[Xiu, Tartakovsky 2006]

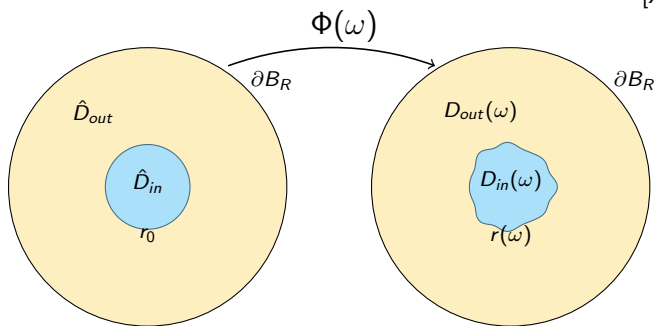


$$-\nabla \cdot (\alpha \nabla u) - \kappa_0^2 n u = 0 \text{ in } D_{in}(\omega) \cup D_{out}(\omega)$$

Numerical realization: forward solver

Random PDE on fixed geometry \longleftrightarrow *Fixed PDE on random geometry*

[Xiu, Tartakovsky 2006]



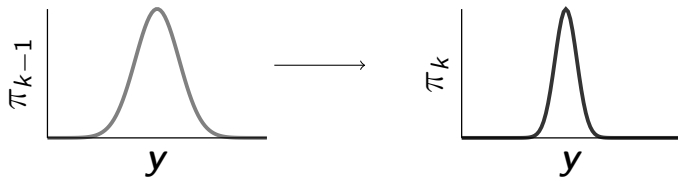
$$-\hat{\nabla} \cdot \left(\hat{\alpha}(\omega) \hat{\nabla} \hat{u} \right) - \kappa_0^2 \hat{n}(\omega) \hat{u} = 0 \text{ in } \hat{D}_{in} \cup \hat{D}_{out}$$

We solve on reference configuration with h -FEM and Perfectly Matched Layer

Numerical realization: SMC sampler

Approximate $\pi_k(\mathbf{y}|\boldsymbol{\delta}) \propto L(\boldsymbol{\delta}|\mathbf{y})^{\gamma_k} \pi_0(\mathbf{y})$ by $\pi_k(\mathbf{y}|\boldsymbol{\delta}) \approx \sum_{p=1}^P W_p^k \delta_{\mathbf{y}_p}(\mathbf{y})$ sequentially.

For $0 < \gamma_1 < \dots < \gamma_K = 1$:



- ① **Reweigh** (update distribution)
- ② **Resample** (if needed, improve representation)
- ③ **MCMC** moves (reintroduce diversity)

Numerical realization: adaptivity in SMC

Selection of **inverse temperatures** [Latz et al. '18]:

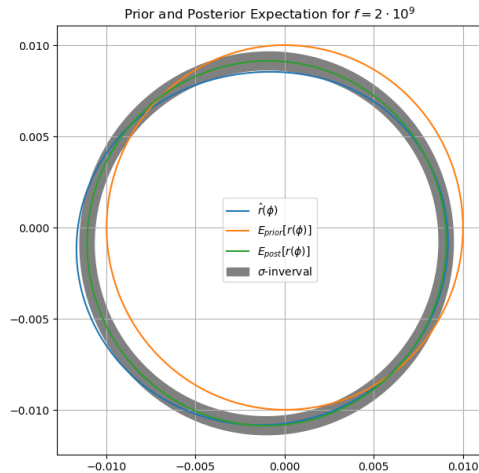
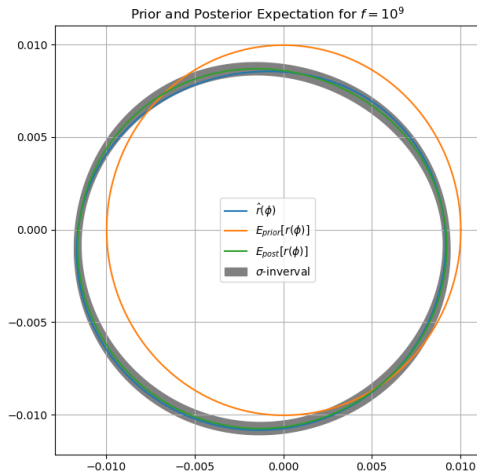
choose largest $\gamma_k \in (\gamma_{k-1}, 1]$ ensuring a given ESS (bisection algorithm).

Variance in random walk Metropolis Hastings [Beskos et al. '15]:

$$\varepsilon_{j,k}^2 = \lambda_k \widehat{\text{Var}}(Y_{j,k}), \quad j = 1, \dots, J,$$

and λ_k adjusted according to acceptance ratio at $(k - 1)$ -th iteration.

Numerical results



Conclusions and extensions

UQ for time-harmonic wave propagation has numerical and statistical challenges

Recent PDE results allow to state **frequency-explicit** posterior stability

Stability constant **grows with frequency**

Similar results hold for **sound-soft** obstacle scattering

Possible extension to full **Maxwell equations**

Possible implications for **imaging**